

Enamel defects of Axenfeld-Rieger syndrome and the role of PITX2 in its pathogenesis

Yi Yang¹  | Junxia Zhu¹  | Yuta Chiba² | Satoshi Fukumoto^{2,3} |
Man Qin¹ | Xin Wang¹ 

¹Department of Pediatric Dentistry, Peking University School and Hospital of Stomatology, Beijing, China

²Division of Oral Health, Section of Oral Medicine for Children, Growth and Development, Faculty of Dental Science, Kyushu University, Fukuoka, Japan

³Division of Pediatric Dentistry, Department of Oral Health and Development Sciences, Tohoku University Graduate School of Dentistry, Sendai, Japan

Correspondence

Xin Wang, Department of Pediatric Dentistry, Peking University School and Hospital of Stomatology, 22 Zhongguancun Avenue South, Haidian District, Beijing 100081, China.
Email: pkussswangxin@bjmu.edu.cn

Funding information

National Clinical Key Discipline Construction Project, Grant/Award Number: PKUSSNMP-201904; Natural Science Foundation of Beijing Municipality, Grant/Award Number: 7164311; Beijing Natural Science Foundation

Abstract

Objectives: To investigate the detailed ultrastructural patterns of dental abnormalities affected by Axenfeld-Rieger syndrome (ARS) with a heterozygous microdeletion involving paired-like homeodomain 2 (*PITX2*) and explored the underlying molecular mechanisms driving enamel defects.

Subjects and methods: Sanger sequencing, genomic quantitative PCR analysis, and chromosomal microarray analysis (CMA) were used to screen the disease-causing mutation in one ARS proband. An exfoliated tooth from an ARS patient was analyzed with scanning electron microscopy and micro-computerized tomography. A stable *Pitx2* knockdown cell line was generated to simulate *PITX2* haploinsufficiency. Cell proliferation and ameloblast differentiation were analyzed, and the role of the Wnt/ β -catenin pathway in proliferation of ameloblast precursor cells was investigated.

Results: An approximately 0.216 Mb novel deletion encompassing *PITX2* was identified. The affected tooth displayed a thinner and broken layer of enamel and abnormal enamel biomineralization. *PITX2* downregulation inhibited the proliferation and differentiation of inner enamel epithelial cells, and LiCl stimulation partially reversed the proliferation ability after *Pitx2* knockdown.

Conclusions: Enamel formation is disturbed in some patients with ARS. *Pitx2* knockdown can influence the proliferation and ameloblast differentiation of inner enamel epithelial cells, and *PITX2* may regulate cell proliferation via Wnt/ β -catenin signaling pathway.

KEYWORDS

axenfeld-rieger syndrome, copy number variation, enamel defects, *PITX2*, Wnt/ β -catenin signaling pathway

1 | INTRODUCTION

Axenfeld-Rieger syndrome (ARS) is a group of rare autosomal dominant human diseases with an incidence of 1 in 200,000. Patients with ARS exhibit specific abnormalities in the anterior segment of the eye, with or without systemic manifestations (Hjalt & Semina, 2005). The major systemic malformations of ARS involve dental, umbilical, heart, and craniofacial abnormalities (Tümer &

Bach-Holm, 2009). Apart from its clinical complexity, ARS also shows a wide range of genetic heterogeneity. Paired-like homeodomain 2 (*PITX2*) and forkhead box C1 (*FOXC1*) are two genes associated with the pathogenesis of ARS (D'Haene et al., 2011), and point mutations or copy number variations of these two genes may cause ARS. Interestingly, ARS patients with systemic abnormalities, especially dental phenotypes, usually have *PITX2* mutations (Tümer & Bach-Holm, 2009). Hypodontia, microdontia, and crossbite

are the main dental manifestations of ARS (Dressler et al., 2010; Waldron et al., 2010). Higher rate of agenesis was seen in the maxilla than in the mandible of patients with ARS (Fan et al., 2019). Enamel defects have been observed in patients with *PITX2* point mutations (Li, Venugopalan, Cao, Pinho, & Paine, 2014a; O'Dwyer & Jones, 2005), but there is a lack of detailed information on the patterns of these defects. The role of *PITX2* in the pathogenesis of enamel anomalies is not fully understood.

Enamel is the only hard tissue that is derived from epithelial origin under physiological conditions (Lacruz et al., 2017). During tooth development, dental epithelial cells proliferate and subsequently differentiate into four distinct cell types, including inner enamel epithelium (IEE) cells, stratum intermedium cells, stellate reticulum cells, and outer enamel epithelium cells under the reciprocal signaling interactions with the mesenchyme. IEE cells are ameloblast progenitor cells, a unique cell population that would further differentiate and transform into secretory ameloblasts and mature ameloblasts, which form an enamel layer with pre-determined metrics of thickness and hardness (Lacruz et al., 2017). The proliferation and ameloblast differentiation of IEE cells are precisely regulated by several transcription factors and signaling molecules, abnormalities in these processes may cause enamel defects.

PITX2 is a member of the paired-like homeobox transcription factor family and has multiple functions during embryonic development. *Pitx2*^{-/-} knockout mouse models resulted in embryonic lethality, and caused developmental malformations in eyes, teeth, heart, and pituitary (Lin et al., 1999; Lu et al., 1999). Global loss of *Pitx2* resulted in arrested tooth development at the placode or bud stage (Lin et al., 1999; Lu et al., 1999). During tooth development, *PITX2* is one of the earliest epithelial markers and is expressed in multiple stages of tooth development in dental epithelia (Hjalt et al., 2000; Mucchielli et al., 1997). *PITX2* also plays an important role in enamel formation. The expression of amelogenin (Amel), the majority of enamel protein, was significantly decreased in the lower incisor of *Pitx2*^{+/-} mice (Li, Venugopalan, Cao, Pinho, & Paine, 2014a). *PITX2* was also shown to bind to the distal promoter of *Amel* and activated *Amel* expression in LS-8 cells, a mouse derived ameloblast-like cell line (Li, Venugopalan, Cao, Pinho, Paine, et al., 2014b). Moreover, inducible inactivation of *PITX2* in adult mice led to disruption of enamel rod organization (Yu et al., 2020).

The Wnt/ β -catenin pathway plays a vital role in tooth development (Liu et al., 2008). The Wnt/ β -catenin pathway is activated sequentially in tooth-forming regions at all tooth developmental stages. Prolonged activation of Wnt/ β -catenin signaling in post-natal mice caused increased proliferation of incisor tooth cervical loop cells and ectopic enamel structure formation (Liu et al., 2010). Interactions between the Wnt/ β -catenin pathway and *PITX2* are involved in the development of several embryonic organs and tissues (Kioussi et al., 2002; Zacharias & Gage, 2010). Deletion of β -catenin in the neural crest resulted in cardiac outflow abnormalities, similar to that seen in *Pitx2*^{-/-} mice (Kioussi et al., 2002). Furthermore, *Pitx2* expression in the fourth branchial arches was decreased in β -catenin conditional knockout mice. Intraperitoneal injection of LiCl

to the *Pitx2*^{+/-} mother resulted in increased *Pitx2* expression in the *Pitx2*-expressing organs in *Pitx2*^{+/-} heterozygous embryos (Kioussi et al., 2002). In a SKOV3 cell line model, *PITX2* was shown to interact with and regulate *WNT2/5a*, which activated the Wnt/ β -catenin pathway and enhanced cell proliferation (Basu & Roy, 2013). In the dental epithelia, nuclear β -catenin expression was decreased in *Pitx2* conditional knockout mice (Yu et al., 2020). However, whether the Wnt/ β -catenin pathway interacts with *PITX2* in enamel formation remains unclear.

In this study, we examined the histology and ultrastructure of dental enamel affected by ARS with a heterozygous microdeletion involving *PITX2* and explored the underlying pathogenic mechanism of copy number variation of *PITX2* on enamel defects.

2 | MATERIALS AND METHODS

2.1 | Subjects and samples

The study protocol was approved by the Ethics Committee of Peking University School and Hospital of Stomatology (PKUSSIRB-2016113122011). The study enrolled a Chinese family with a child diagnosed with ARS. Informed consent was obtained from the subject's guardian. The proband was clinically diagnosed with ARS by an ophthalmologist. Clinical and radiographic examinations were performed and 4 ml of peripheral blood was drawn for analysis.

The exfoliated right primary mandibular incisor was collected from the ARS patient with a different heterozygous microdeletion involving *PITX2*, as previously reported (Yang et al., 2018). Two extracted primary mandibular incisors from two healthy children of the same age due to primary tooth retention were used as normal controls.

2.2 | Gene sequencing, genomic quantitative PCR analysis (qPCR), and chromosomal microarray analysis (CMA)

Genomic DNA was extracted using a TIANamp Blood DNA minikit (Tiangen, Beijing, China) according to the manufacturer's instructions. The *PITX2* gene was amplified by PCR using TaKaRa Ex Taq (Takara Bio.), and the products were purified and sequenced using an ABI 377 Automatic Sequencer (Applied Biosystems.). All DNA sequences were analyzed using Mutation Surveyor (SoftGenetics.). The primer sequences used are shown in supporting information Table S1.

DNA quantitative PCR was carried out in triplicate for *PITX2* using the ABI Prism 7500 Real-Time PCR System (Applied Biosystems) and SYBR Green Master Mix (Roche Diagnostics.). The gene expression levels were normalized to levels of *GAPDH*. The primer sequences used to amplify exon 1 or exon 8 of *PITX2* are summarized in supporting information Table S2.

The CytoScan HD array platform (Affymetrix,) was applied to validate the deletions and to determine the exact genomic location of the deleted regions. The entire procedure was performed as previously reported (Yang et al., 2018).

2.3 | Micro-computerized tomography

A micro-computerized tomography scanner (GANTRYSTD CT 3121; Siemens) was used to scan all teeth with 80kV, 500 μ A. Raw data obtained were reconstructed using the Inveon Research Workplace 4.2 software (Siemens). Enamel and dentine were defined by specific radiopacity (radiodensity) values, with enamel being more radiopaque than dentine. We chose 9 points in the labial and lingual side of the teeth (Figure 2C) to measure the enamel thickness.

2.4 | Scanning electron microscopy (SEM) and energy dispersive spectrometry (EDS)

After sectioning and polishing, tooth specimens for SEM (SU8010, HITACHI) were etched with 37% phosphoric acid for 60s, and all specimens were washed with distilled water for 60s. The surfaces of the specimens were sputter-coated with gold after vacuum-drying. Microstructural analysis was carried out by SEM, operated at 5.0 kV. The EDS results were performed using XFlash6130 (Bruker, Germany). Elemental measurements (Ca, O, P, C) were conducted at three points in the enamel: labial, lingual, and incisal edge.

2.5 | Cell culture and transfection

The rat incisor-derived dental epithelial cell line, SF2, was kindly provided by Professor Satoshi Fukumoto (Tohoku University Graduate School of Dentistry,). The SF2 cell line is a preameloblast cell line and has the potential to differentiate into ameloblasts (Arakaki et al., 2012). SF2 cells were cultured in Dulbecco's modified Eagle's medium DMEM/F-12 (Invitrogen,) supplemented with 10% fetal bovine serum (FBS) in a humidified atmosphere at 37°C with 5% CO₂.

Two lentivirus-shRNAs (sh-*Pitx2*#1/2) that effectively targeted *Pitx2* and one unrelated control (scramble) were custom-made by Genechem (Shanghai, China); targeted sequences are shown in supporting information Table S3. For the transfection experiments, SF2 cells were seeded in 6-well plates at a density of 2 \times 10⁵ cells/well and grown for 16h. The cells were transfected with the sh-*Pitx2*#1/2 or scramble at a multiplicity of infection (MOI) of 50. After 12h of transfection, the medium was replaced. After 48h, transfected cells were cultured in the presence of 5 mg/mL polybrene. The knock-down efficiency was evaluated using fluorescence microscopy, reverse-transcription quantitative polymerase chain reaction (RT-qPCR), and western blot analysis. Lithium chloride (LiCl; Solarbio,)

an agonist of the Wnt- β -catenin signaling pathway was added at 500nM in the rescue experiments.

2.6 | CCK8 assay

SF2 cells transfected with either the sh-*Pitx2* or the scramble were seeded in 96-well plates at a density of 2 \times 10³ cells/well and cultured overnight. Cell proliferation was then examined using the Cell Counting Kit-8 (CCK-8; Dojindo,) on days 1, 2, 3, and 4. Afterwards, 10 μ l CCK-8 reagent was added into each well, and the cells were incubated for 1 h at 37°C in the dark. Absorbance at 450nm was measured in a microplate reader (Thermo 3001, Thermo,) to determine the number of live cells in each well.

2.7 | EdU staining

Proliferation of SF2 cells was also investigated with BeyoClick™EdU Cell Proliferation Kit (C0075S, Beyotime,) according to the manufacturer's protocols. The images were captured with a fluorescence microscope (Olympus,). SF2 cells that undergo DNA replication during the incubation present red fluorescence, while the nucleus is indicated by blue fluorescence. The EdU-positive ratio was calculated using ImageJ software (National Institutes of Health,).

2.8 | Alizarin red staining

SF2 cells were seeded in 6-well plates at a density of 2 \times 10⁵ cells/well and cultured in DMEM/F12 with 10% FBS and 5 mg/mL polybrene until cells reached 80%–90% confluence. Then the medium was replaced with DMEM/F12 containing 10% FBS, 5 mg/mL polybrene, 10mM β -glycerophosphate, 10 nM dexamethasone, and 50 μ g/mL ascorbic acid. After induction for 1week, alizarin red stain was applied to evaluate mineralization. Cells were fixed with 4% paraformaldehyde for 10 min and then stained for 30min with 2% ARS (Sigma-Aldrich Co., St Louis, MO, USA). Subsequently, 10% cetylpyridinium chloride was added to dissolve the modules for 15 min. The absorbance of 100 μ l of the supernatant was measured at 562nm using a microplate reader (Thermo 3001, Thermo).

2.9 | Quantitative RT-PCR (RT-qPCR)

Total RNA was extracted using TRIzol Reagent (Invitrogen,) according to the manufacturer's instructions. Total RNA was reverse-transcribed using the Prime Script First-Strand cDNA Synthesis Kit (TaKaRa Biotechnology,), and RT-qPCR was carried out with SYBR Green Master Mix (Roche Diagnostics,) in an ABI Prism 7500 Real-Time PCR System (Applied Biosystems). Gene expression was quantified using the 2^{- $\Delta\Delta$ Ct} method and normalized to *Gapdh* mRNA levels. The sequences of the primer pairs used for quantitation of

Pitx2, *Gapdh*, *Amel*, *Alp*, *Ambn*, *c-Myc*, and β -catenin mRNA expression are listed in supporting information Table S4.

2.10 | Western blot analysis

Total protein was extracted using RIPA buffer (Solarbio,) supplemented with protease inhibitors. Cytoplasmic and nuclear proteins were extracted with Nuclear and Cytoplasmic Extraction Reagents P1200 (Applygen,) according to the manufacturer's protocol. Protein samples were separated using SDS-PAGE in a 10% gel and then transferred to a PVDF membrane at 200 mA for 2 h. The membranes were blocked for 1 h with 5% skim milk and incubated overnight at 4°C with primary antibodies: anti-PITX2 (1:8000; Proteintech), anti-GAPDH (1:10000; Proteintech), anti- α -Tubulin (1:10000; Proteintech), anti-c-MYC (1:1000; Proteintech), anti- β -catenin (1:10000; Proteintech), and anti-Lamin A/C (1:10000; Proteintech) antibodies. The next day, the membranes were incubated for 1 h at 37°C with the corresponding secondary antibodies (1:10000; Proteintech), and the immunoreactive protein bands were visualized with an ECL Kit (Solarbio, Beijing) according to the manufacturer's instructions. Densitometric analysis of protein expression was calculated using ImageJ software.

2.11 | Statistical analyses

Results presented as means \pm standard deviation (SD) were represented at least three independent replicates. A two-tailed student's t test was applied for statistical analysis of two independent variables. Data with three or more variables were analyzed using one-way analysis of variance (ANOVA). GraphPrism9 statistical software (GraphPad Software) was used for all statistical analyses. A p value <0.05 was considered statistically significant.

3 | RESULTS

3.1 | A novel disease-causing CNV encompassing PITX2 identified in a Chinese patient with ARS

The proband was a 7-year-old girl presenting with abnormalities in the eyes, teeth, and umbilicus (Figure 1a). Dental and radiographic examinations revealed severe hypodontia, crossbite, and midface deficiency (Figure 1b,c,d). No obvious enamel defects were observed in proband's untreated teeth, while multiple caries and fillings were detected. Telecanthus was presented in the proband (Figure S1). Schwalbe's line was prominently visible and displaced anteriorly in both eyes (Figure S1). And iridocorneal adhesions were also observed. Fundoscopy showed the cup-to-disk ratio was 0.4 and 0.6 in the right and left eye, respectively (Figure S1). The intraocular pressure (IOP) in her right eye was 24.1 mmHg and 34.8 mmHg in her left eye. Secondary glaucoma was also diagnosed. Umbilical stump of the proband was abnormally protruding (Figure S1). Initially, gene

sequencing of proband found no disease-related mutation in the *PITX2* gene, and the genotypes of all SNP loci evaluated were detected as homozygotic. Then, following the screening method we established in our previous study (Yang et al., 2018), a novel heterozygous deletion involving *PITX2* was discovered and confirmed by qPCR and CMA (Figure 1e,f). The length of the deletion segment was about 0.216 Mb (chr4:111, 437, 127–111, 652, 876, GRCh37/hg19) involving the *PITX2* and *ENPEP* genes (Figure 1f).

3.2 | Enamel defects in the patient with ARS

Compared with the normal control, tooth wear in the exfoliated tooth from the patient with ARS was milder and the dental crown was smaller, with obtuse mesial and distal labial angles (Figure 2a). Enamel thickness analysis revealed an extremely thin enamel layer in the labial and lingual sides of the ARS sample (Figure 2b,c,d,e). Unlike the normal control, increased broken and collapsed rods were observed in the ARS sample (Figure 2f). The percentages of Ca and P content were both significantly lower in the ARS sample compared to the control sample ($p < 0.05$, Tables 1), but there was no statistically significant difference in either O or C components ($p > 0.05$, Table 1).

3.3 | PITX2 downregulation inhibits the proliferation and differentiation of dental epithelial cells

To simulate *PITX2* haploinsufficiency and explore its impact on cell bio-behaviors, we analyzed the cell proliferation and differentiation in control and *Pitx2*-knockdown SF2 cells. The infection efficiency of shRNA lentivirus was verified by fluorescence microscopy, and over 90% of the transfected SF2 cells expressed GFP (Figure 3a). Compared to scramble transfected cells, the levels of *PITX2* mRNA and protein were both greatly decreased in the sh-*Pitx2*#1/2 transfected cells (Figure 3b,c,d,e). Cells transfected with sh-*Pitx2*#2 were used in subsequent experiments, due to its higher knockdown efficiency (named as sh-*Pitx2* in the later manuscript). To rule out target-off effects, CCK-8 assay and Alizarin red staining were repeated in sh-*Pitx2*#1/2 transfected cells (supporting information Figure S2).

In the CCK-8 assay, transfection of SF2 cells with sh-*Pitx2* resulted in a much lower proliferation (Figure 4a). Similar results were observed in EdU staining assays (Figure 4b). The ratio of EdU-positive cells was significantly decreased after knockdown of *Pitx2* (Figure 4b,c).

We further investigated the effects of *Pitx2* knockdown on the ability of SF2 cells to differentiate into ameloblasts. The expression levels of ameloblast differentiation marker genes *Amel*, *Alp*, and *Ambn* were all notably decreased, as determined by RT-qPCR (Figure 4d). Alizarin red staining also revealed that the mineralized nodule formation was disrupted in sh-*Pitx2* transfected cells (Figure 4e,f). These findings suggested that SF2 cell proliferation and ameloblast differentiation ability were affected by downregulation of *PITX2*.

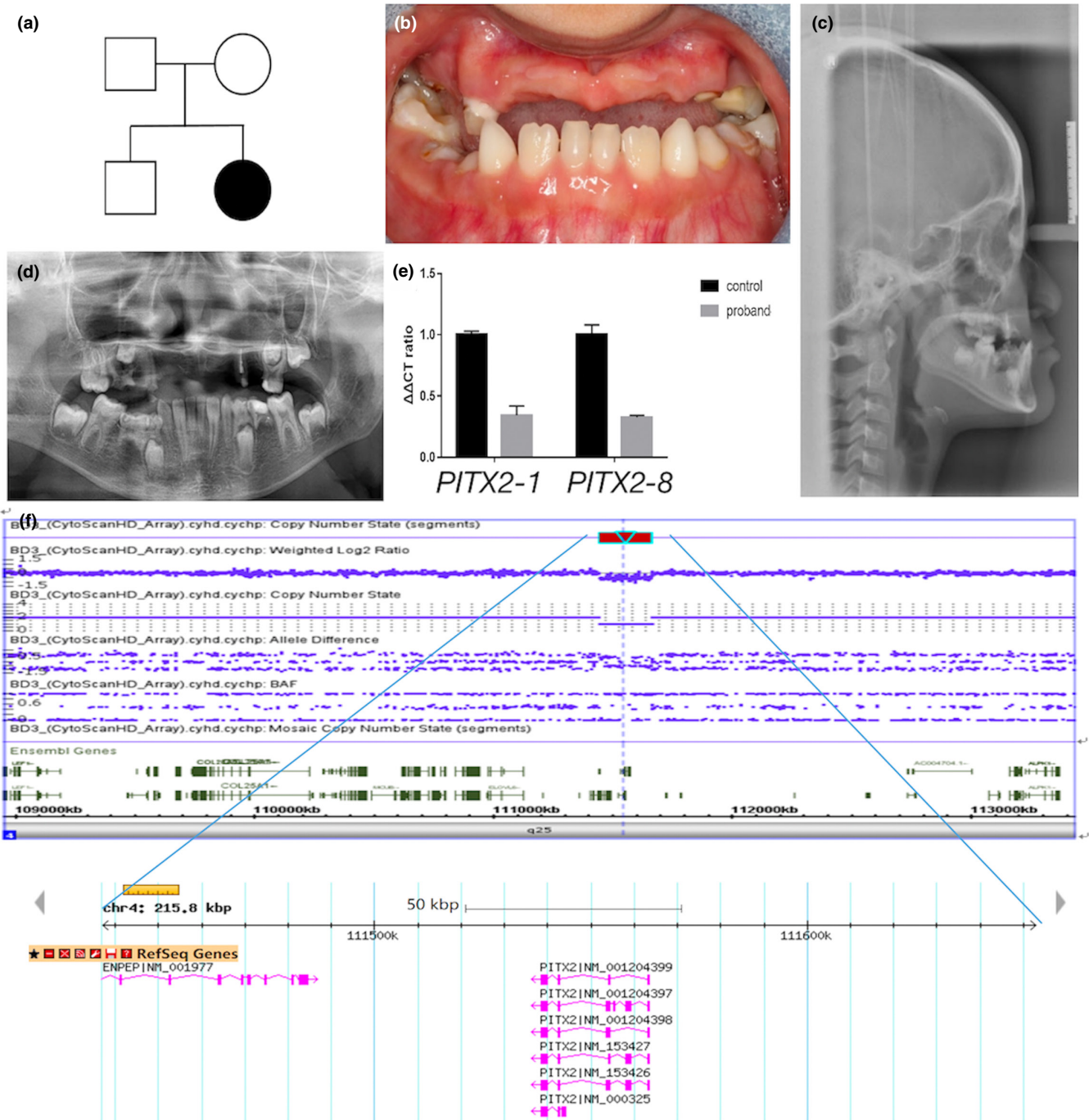


FIGURE 1 The recruited family with a novel CNV involving *PITX2*. (a) Pedigree of the family. (b) Intraoral view of the proband. (c) Lateral cephalogram of the proband. (d) a panoramic radiograph of the proband. (e) a microdeletion encompassing *PITX2-1* and *PITX2-8* was verified by qPCR. (f) an approximately 0.216 mb (chr4:111, 437, 127–111, 652, 876, GRCh37/hg19) deletion including two genes (*PITX2* and *ENPEP*) was identified in the proband using CMA

3.4 | *PITX2* downregulation may affect cell proliferation via Wnt/β-catenin signaling pathway

The Wnt/β-catenin signaling pathway is crucial for cell proliferation. Disruption of the Wnt/β-catenin pathway could result in impaired proliferation of epithelial cells and pre-odontoblasts. β-catenin is a central component of the Wnt/β-catenin signaling pathway, and stabilization and nuclear accumulation of β-catenin can activate the expression of

Wnt target genes such as *c-MYC* and *cyclin D1*. To test whether the Wnt/β-catenin signaling pathway is affected by *Pitx2* knockdown in SF2 cells, we examined the expression of major components in this pathway. Western blot analyses showed that total β-catenin levels and expression of the downstream proliferation marker *c-MYC* were significantly lower in sh-*Pitx2* transduced SF2 cells (Figure 5a,b,c).

LiCl activates the Wnt/β-catenin signaling pathway. Using RT-qPCR and western blot, we found that the mRNA and protein

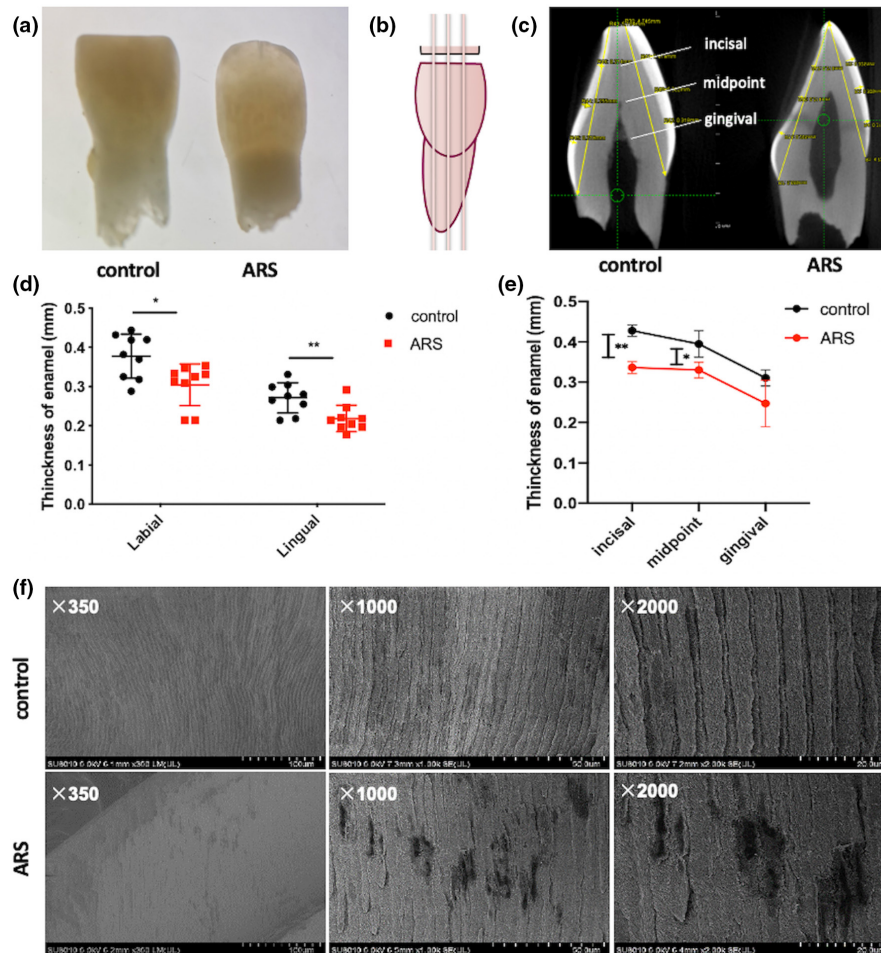


FIGURE 2 (a) Clinical observation of teeth from the healthy control and the patient with ARS (information published previously). (b) the diagram of enamel thickness measurement. The incisal edge of the tooth was divided into four equal parts by three points, three sections across these points that were parallel to the long axis of the tooth and perpendicular to the incisal edge were made. At the sagittal plane of each section (c), two lines were made from the incisal edge to the enamel-cementum junction (edge-enamel-cementum line). Each line was divided into four equal parts and a hypothetical vertical line was made perpendicular to the edge-enamel-cementum line at each equal point and enamel thickness on the hypothetical vertical line were then measured. A total of 9 points of enamel thickness on the labial or lingual side were obtained for each tooth. (c) Severe attrition in the control teeth. (d) the enamel of the healthy control was significantly thicker than that of affected tooth on both labial and lingual surfaces. (e) the site-specific enamel thickness on the labial surface was measured. The enamel of the healthy control was significantly thicker at incisal and midpoint sites in comparison to that of the affected tooth. (f) SEM images of the healthy control and the ARS patient teeth. (** $p < 0.01$ and *** $p < 0.001$)

TABLE 1 Comparison of elemental content of affected teeth (ARS) vs. unaffected teeth (control) (wt % + SD)

Mineral	Control	ARS	<i>p</i>
Ca	41.78 + 1.636	26.66 + 1.64	0.0009***
O	40.42 + 5.351	48.42 + 0.8572	0.1110
P	14.9 + 0.896	10.46 + 0.40	0.0019**
C	7.46 + 0.5925	14.45 + 2.761	0.1083

wt: weight;

** $p < 0.01$ and *** $p < 0.001$.

expression of β -catenin and c-MYC were significantly increased when sh-Pitx2 transduced SF2 cells were treated with LiCl (Figure 6b,c,d). Concomitantly, CCK-8 assay validated that sh-Pitx2 transfected SF2 cells had significantly increased proliferation on days 2 and 3 after

adding LiCl (Figure 6a). Thus, our findings indicate that the loss of PITX2 may affect the proliferation of SF2 cells via the Wnt/ β -catenin signaling pathway.

4 | DISCUSSION

Copy number variation (CNV) is a source of genetic diversity in humans. Like single nucleotide polymorphisms (SNP), CNV can represent benign polymorphic variations or can cause genetic diseases (Lauer & Gresham, 2019). ARS can be caused by CNV of PITX2, which accounts for at least 30% of ARS cases exhibiting dental and umbilical anomalies (Reis et al., 2012). Before high-throughput sequencing technologies have been broadly applied, it was difficult to detect CNVs in patients with genetic diseases. Even with the invent

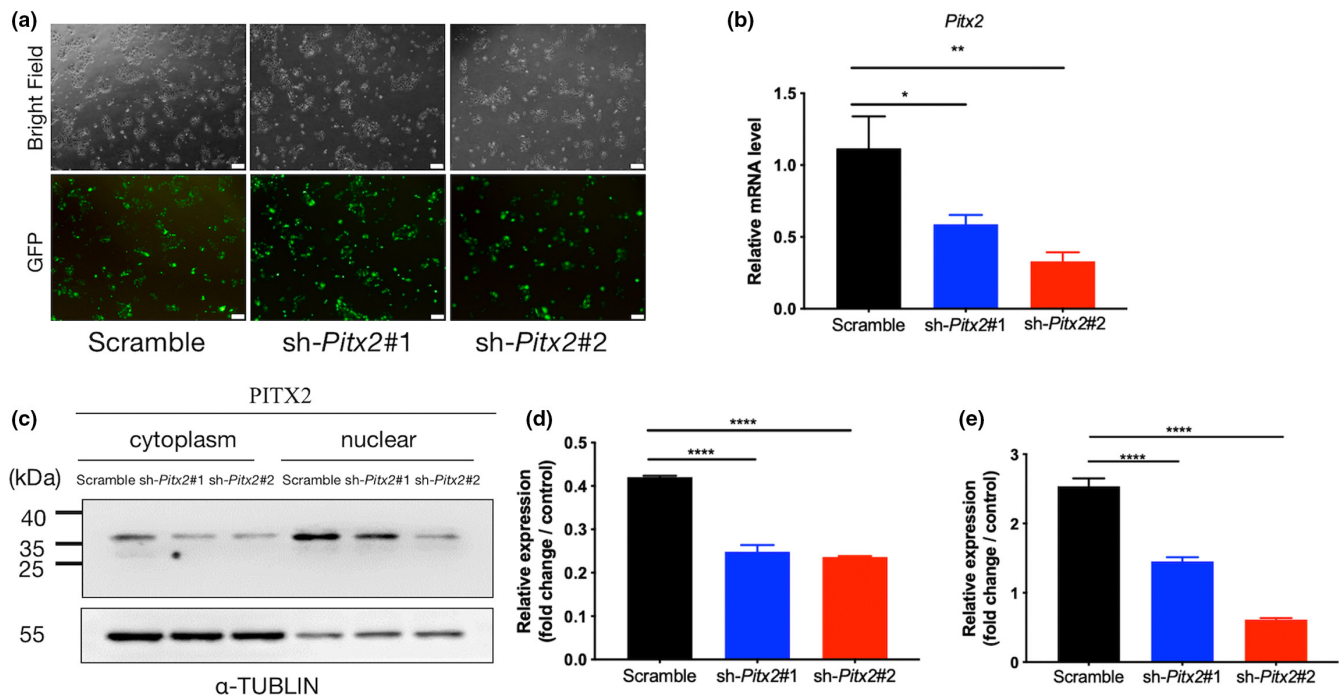


FIGURE 3 Stable *Pitx2* knockdown in SF2 cells. (a) Representative bright-field (top) and fluorescence (bottom) microscopy images illustrating the proportion of cells expressing GFP, as an indicator of infection efficiency. Scale bars, 200 μ m. (b) Histograms of the relative levels of *Pitx2* mRNA in transfected SF2 cells. (c) Representative western blots showing the protein level of PITX2 in SF2 cells. (d) Densitometric analysis of PITX2 expression in the cytoplasm. (e) Densitometric analysis of PITX2 expression in the nucleus. (* $p < 0.05$, ** $p < 0.01$ and **** $p < 0.0001$)

of next-generation sequencing (NGS)-based CNV analysis, it is still considered to be a relatively low cost-effective way in discovering this type of variation. In our previous study (Yang et al., 2018), we established an effective sequencing protocol that helped recognize and verify the existence of a disease-causing CNVs. Initially, when we tried to screen the *PITX2* gene of the proband in the present study, no disease-associated mutations were found by Sanger sequencing. However, the genotypes of several frequently occurring SNP loci were detected as homozygous in the proband, which indicated that there might be a large segment deletion encompassing these SNP loci. Subsequently, a novel heterozygous deletion involving *PITX2* was ultimately discovered and fine-mapped through qPCR and CMA. This suggests that SNP genotypes within a candidate gene may have a potential for predicting the existence of a large segment deletion in autosomal dominant diseases.

The main craniofacial and dental phenotypic characteristics of ARS include hypodontia, crossbite, and midface hypoplasia (Simone Dressler et al., 2010). Hypoplasia of the enamel, taurodontism, and hyperplastic maxillary labial frenum have also been observed (O'Dwyer & Jones, 2005). To date, studies mostly focused on hypodontia and eye defects, the two most prominent clinical manifestations of ARS, whereas the patterns of enamel defects in ARS patients have been rarely documented. In this study, we obtained one primary mandibular incisor from an ARS patient, described previously, with a heterozygous deletion involving *PITX2*. A smaller-sized crown and a thinner layer of enamel with reduced calcium and phosphorus contents was found. Irregular, broken, and collapsing

enamel rods were also observed by SEM. These observations suggested an important role of *PITX2* during amelogenesis in humans, and was consistent with animal models, as the disruption of the enamel rod organization was detected in *Pitx2* inducible knockout mice (Yu et al., 2020). Considering cell proliferation and dental epithelium cell differentiation were compromised in *Pitx2* knockout mice (Yu et al., 2020), we therefore hypothesized that the loss of *PITX2* may affect the proliferation and ameloblast differentiation ability of inner enamel epithelial cells, resulting in the enamel defects found in the patient.

PITX2 is required for promoting cell proliferation in a cell type-specific manner during embryonic development (Baek et al., 2003). Down-regulation of *PITX2* in induced hepatic stem cells (iHepSCs) inhibited cell proliferation (Chen et al., 2016). Conversely, the *PITX2* knockdown increased the proliferation of Caco-2 cells (a colorectal cancer cell line) (Hirose et al., 2011). Our study found that *Pitx2* knockdown suppressed the growth of SF2 cells, which is in concordance with the in vivo observations that epithelial cell proliferation was decreased in *Pitx2* conditional knockout mouse embryos (Yu et al., 2020).

The mutual relationship of *PITX2* and Wnt/ β -catenin has been demonstrated in numerous studies. In the developing pituitary gland, *Pitx2* is a transcriptional target of the canonical Wnt/ β -catenin signaling pathway (Kioussi et al., 2002). Wnt/ β -catenin directly induced *PITX2* and controlled cell proliferation by regulating the expression of genes such as *cyclin D2* and *c-Myc* in C2C12 cells (Baek et al., 2003). *PITX2* could activate the canonical Wnt pathway as well and was

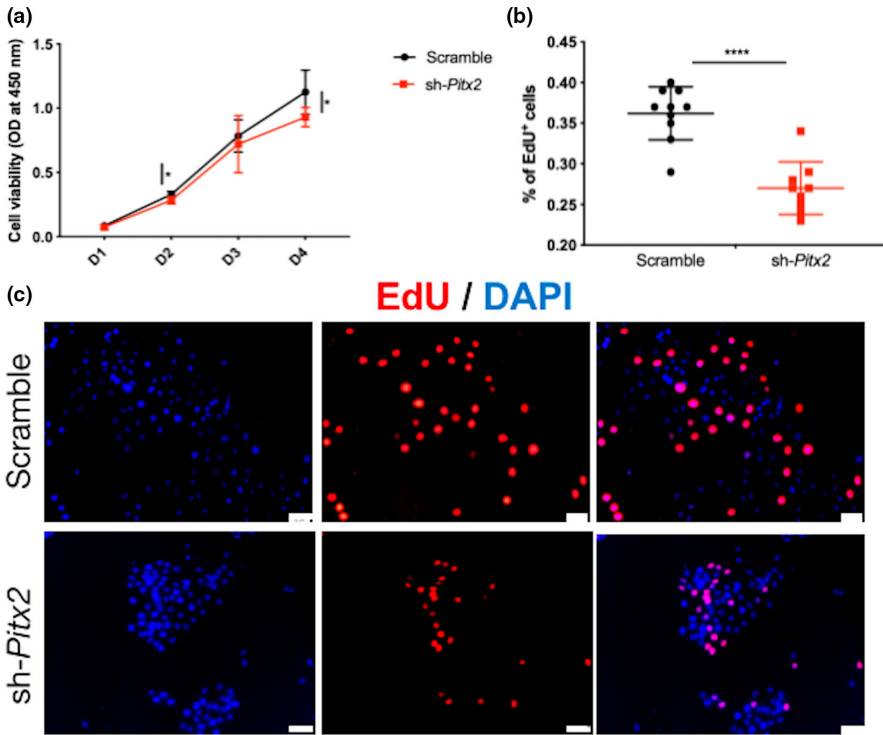


FIGURE 4 *Pitx2* knockdown inhibited the proliferation and ameloblast differentiation of inner enamel epithelial cells. (a) Cell proliferation was evaluated using the CCK-8 assay. (b) the percentage of EdU-positive cells in the two groups. (c) Representative fluorescence images of Edu staining of SF2 cells. Scale bars, 50 μm. (d) the relative expression of *Alpl*, *Amel*, and *Ambn* after *Pitx2* knockdown (**p* < 0.05 and *****p* < 0.0001). (e) Alizarin red staining of SF2 cells. Scale bars, 100 μm. (f) Quantitative measurements of mineralized nodules evaluated by alizarin red staining (***p* < 0.01)

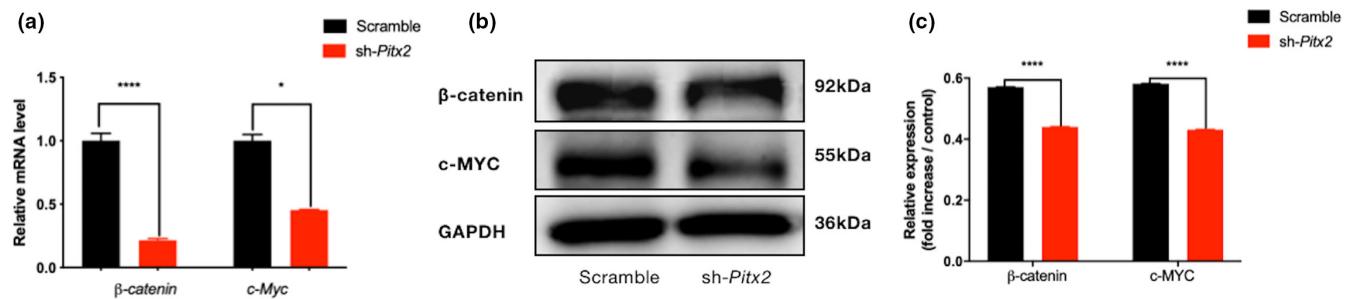
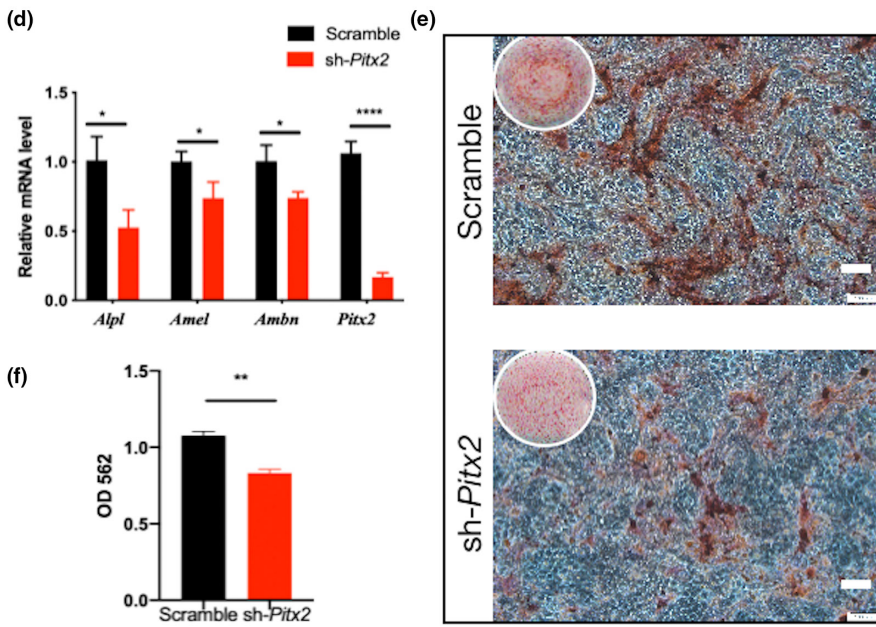


FIGURE 5 The Wnt/β-catenin signaling pathway was affected in *Pitx2* knockdown cells. (a) qRT-PCR and (b,c) western blot analysis showing the expression of β-catenin and c-MYC after *Pitx2* knockdown in SF2 cells

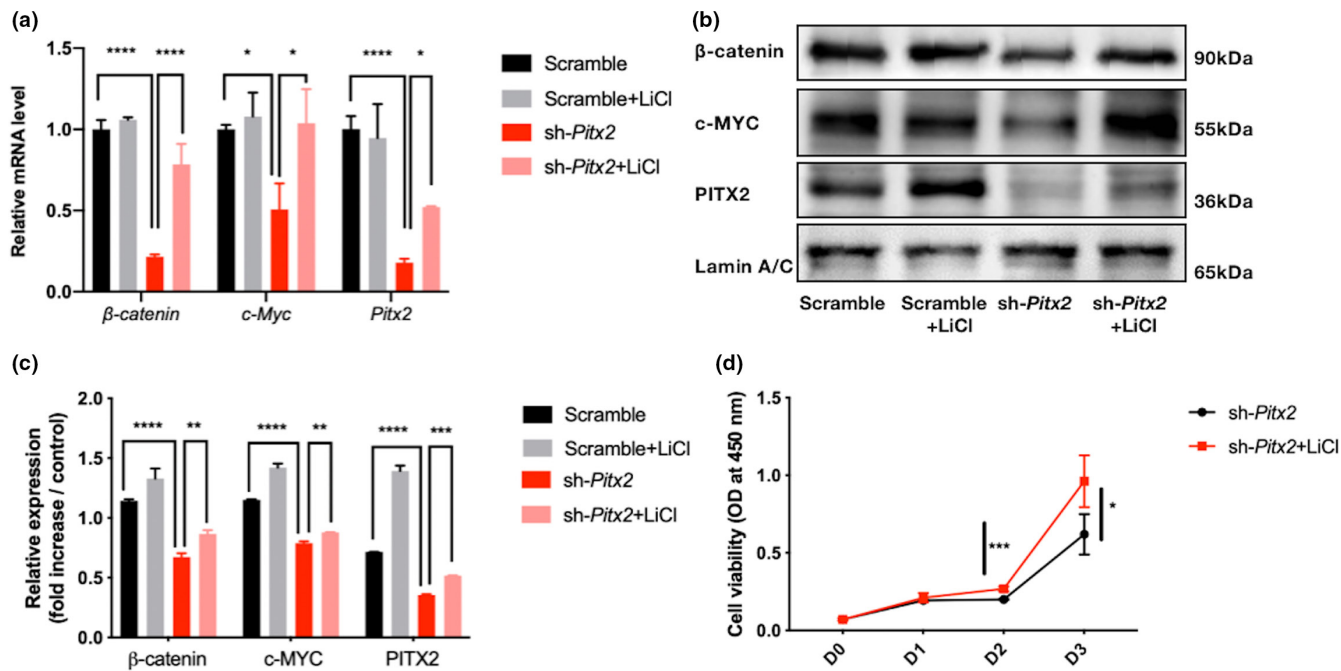


FIGURE 6 PITX2 regulated cell proliferation via the Wnt- β -catenin pathway. LiCl stimulation partially reversed the suppression of β -catenin, c-MYC, and PITX2 at the (a) mRNA and (b,c) protein levels. (D) Cell proliferation of sh-Pitx2 transfected SF2 cells was enhanced in the presence of 500nM LiCl

shown to promote proliferation in SKOV-3 cells, through inducing Wnt ligands. Yu et al. reported that the Wnt canonical pathway was attenuated in *Pitx2* knock out mice (Yu et al., 2020). Consistent with these studies, we found that the expression levels of both β -catenin and c-MYC, a downstream target of the Wnt/ β -catenin pathway, were decreased after *Pitx2* knockdown in SF2 cells. Stimulation with LiCl partially reversed the expression of these factors and also increased the proliferation of *Pitx2* knockdown SF2 cells. These findings demonstrated the close relationship of PITX2 and the Wnt canonical pathway in regulating the proliferation of dental epithelial cells.

Amelogenin and ameloblastin, encoded by *Amel* and *Ambn*, respectively, are the most abundant enamel matrix proteins in amelogenesis and are responsible for regulating crystal shape and crystal growth and for maintaining ameloblast differentiation (Fukumoto et al., 2005; Shin et al., 2020). Tissue-nonspecific alkaline phosphatase isozyme (TNAP, ALPL) has long been associated with the cells of mineralizing tissues, such as cartilage, bone, and teeth, and is highly expressed in ameloblasts during the maturation stages (Yadav et al., 2012). Previous studies found that PITX2 binded to the distal promoter of *Amel* and activated *Amel* expression. However, ARS-causing PITX2 mutants failed to activate the *Amel* promoter (Li, Venugopalan, Cao, Pinho, Paine, et al., 2014b). Similarly, in our study, the mRNA expression of ameloblast differentiation markers were decreased after *Pitx2* knockdown. Alizarin red staining showed disrupted mineralized nodule formation in *Pitx2* knockdown cells, providing further evidence that PITX2 is involved in ameloblast differentiation of IEEs, and may regulate enamel formation during tooth development.

Our study is the first effort to investigate the ultrastructural patterns of enamel defects in a patient with ARS. In vitro data demonstrated that *Pitx2* knockdown had an impact on the proliferation and ameloblast differentiation of inner enamel epithelial cells. Our data suggested that PITX2 might regulate cell proliferation via the Wnt/ β -catenin signaling pathway. What we discovered shone a light on the etiology of enamel defects in ARS patients associated with haploinsufficiency of PITX2. It is worthwhile to evaluate additional cases of ARS to explore the connection between genotype and phenotype and to analyze the underlying mechanisms of ARS pathogenesis.

AUTHOR CONTRIBUTIONS

Yi Yang: Data curation; formal analysis; investigation; methodology; writing – original draft. **Junxia Zhu:** Data curation; methodology; writing – review and editing. **Yuta Chiba:** Data curation; methodology; visualization; writing – review and editing. **Satoshi Fukumoto:** Data curation; methodology; resources; visualization; writing – review and editing. **Man Qin:** Conceptualization; funding acquisition; resources; supervision; writing – review and editing. **Xin Wang:** Conceptualization; data curation; formal analysis; funding acquisition; methodology; resources; supervision; writing – review and editing.

ACKNOWLEDGMENTS

The authors are grateful to all study participants for their contributions. This study was supported by grants from the Beijing Natural Science Foundation [grant number 7164311] and National Clinical Key Discipline Construction Project [PKUSSNMP-201904].

FUNDING INFORMATION

Supported by Beijing Natural Science Foundation (7164311) and National Clinical Key Discipline Construction Project (PKUSSNMP-201904).

CONFLICT OF INTEREST

None to declare.

DATA AVAILABILITY STATEMENT

The data that support the findings of this study are available from the corresponding author upon reasonable request.

PEER REVIEW

The peer review history for this article is available at <https://publons.com/publon/10.1111/odi.14315>.

ETHICAL APPROVAL

The study protocol was approved by the Ethics Committee of Peking University School and Hospital of Stomatology (PKUSSIRB-2016113122011).

PATIENT CONSENT STATEMENT

Informed consent was obtained from the subject's guardian.

ORCID

Yi Yang  <https://orcid.org/0000-0003-0173-7306>

Junxia Zhu  <https://orcid.org/0000-0002-6050-0643>

Xin Wang  <https://orcid.org/0000-0001-9658-8694>

REFERENCES

- Arakaki, M., Ishikawa, M., Nakamura, T., Iwamoto, T., Yamada, A., Fukumoto, E., Saito, M., Otsu, K., Harada, H., Yamada, Y., & Fukumoto, S. (2012). Role of epithelial-stem cell interactions during dental cell differentiation. *The Journal of Biological Chemistry*, 287(13), 10590–10601. <https://doi.org/10.1074/jbc.M111.285874>
- Baek, S. H., Kioussi, C., Briata, P., Wang, D. G., Nguyen, H. D., Ohgi, K. A., Glass, C. K., Wynshaw-Boris, A., Rose, D. W., & Rosenfeld, M. G. (2003). Regulated subset of G(1) growth-control genes in response to derepression by the Wnt pathway. *Proceedings of the National Academy of Sciences of the United States of America*, 100(6), 3245–3250. <https://doi.org/10.1073/pnas.0330217100>
- Basu, M., & Roy, S. S. (2013). Wnt/beta-catenin pathway is regulated by PITX2 homeodomain protein and thus contributes to the proliferation of human ovarian adenocarcinoma cell, SKOV-3. *The Journal of Biological Chemistry*, 288(6), 4355–4367. <https://doi.org/10.1074/jbc.M112.409102>
- Chen, F., Yao, H., Wang, M., Yu, B., Liu, Q., Li, J., He, Z., & Hu, Y. P. (2016). Suppressing Pitx2 inhibits proliferation and promotes differentiation of iHepSCs. *The International Journal of Biochemistry & Cell Biology*, 80, 154–162. <https://doi.org/10.1016/j.biocel.2016.09.024>
- D'Haene, B., Meire, F., Claerhout, I., Kroes, H. Y., Plomp, A., Arens, Y. H., de Ravel, T., Casteels, I., De Jaegere, S., Hooghe, S., Wuyts, W., van den Ende, J., Roulez, F., Veenstra-Knol, H. E., Oldenburger, R. A., Giltay, J., Verheij, J. B., de Faber, J. T., Menten, B., ... De Baere, E. (2011). Expanding the spectrum of FOXC1 and PITX2 mutations and copy number changes in patients with anterior segment malformations. *Investigative Ophthalmology & Visual Science*, 52(1), 324–333. <https://doi.org/10.1167/iov.10-5309>. http://www.ncbi.nlm.nih.gov/entrez/query.fcgi?cmd=Retrieve&db=pubmed&dopt=Abstract&list_uids=20881294&query_hl=1
- Dressler, S., Meyer-Marcotty, P., Weisschuh, N., Jablonski-Momeni, A., Pieper, K., Gramer, G., & Gramer, E. (2010). Dental and craniofacial anomalies associated with Axenfeld-Rieger syndrome with PITX2 mutation. *Case Reports in Medicine*, 2010, 621984. <https://doi.org/10.1155/2010/621984>.
- Fan, Z., Sun, S., Liu, H., Yu, M., Liu, Z., Wong, S. W., Liu, Y., Han, D., & Feng, H. (2019). Novel PITX2 mutations identified in axenfeld-rieger syndrome and the pattern of PITX2-related tooth agenesis. *Oral Diseases*, 25(8), 2010–2019. <https://doi.org/10.1111/odi.13196>
- Fukumoto, S., Yamada, A., Nonaka, K., & Yamada, Y. (2005). Essential roles of ameloblastin in maintaining ameloblast differentiation and enamel formation. *Cells, Tissues, Organs*, 181(3–4), 189–195. <https://doi.org/10.1159/000091380>
- Hirose, H., Ishii, H., Mimori, K., Tanaka, F., Takemasa, I., Mizushima, T., Ikeda, M., Yamamoto, H., Sekimoto, M., Doki, Y., & Mori, M. (2011). The significance of PITX2 overexpression in human colorectal cancer. *Annals of Surgical Oncology*, 18(10), 3005–3012. <https://doi.org/10.1245/s10434-011-1653-z>
- Hjalt, T. A., & Semina, E. V. (2005). Current molecular understanding of Axenfeld-Rieger syndrome. *Expert Reviews in Molecular Medicine*, 7(25), 1–17. <https://doi.org/10.1017/S1462399405010082>. http://www.ncbi.nlm.nih.gov/entrez/query.fcgi?cmd=Retrieve&db=pubmed&dopt=Abstract&list_uids=16274491&query_hl=1
- Hjalt, T. A., Semina, E. V., Amendt, B. A., & Murray, J. C. (2000). The Pitx2 protein in mouse development. *Developmental Dynamics*, 218(1), 195–200. [https://doi.org/10.1002/\(SICI\)1097-0177\(200005\)218:1<195::AID-DVDY17>3.0.CO;2-C](https://doi.org/10.1002/(SICI)1097-0177(200005)218:1<195::AID-DVDY17>3.0.CO;2-C)
- Kioussi, C., Briata, P., Baek, S. H., Rose, D. W., Hamblet, N. S., Herman, T., Ohgi, K. A., Lin, C., Gleiberman, A., Wang, J., Brault, V., Ruiz-Lozano, P., Nguyen, H. D., Kemler, R., Glass, C. K., Wynshaw-Boris, A., & Rosenfeld, M. G. (2002). Identification of a Wnt/Dvl/beta-catenin --> Pitx2 pathway mediating cell-type-specific proliferation during development. *Cell*, 111(5), 673–685. [https://doi.org/10.1016/s0092-8674\(02\)01084-x](https://doi.org/10.1016/s0092-8674(02)01084-x)
- Lacruz, R. S., Habelitz, S., Wright, J. T., & Paine, M. L. (2017). Dental enamel formation and implications for Oral health and disease. *Physiological Reviews*, 97(3), 939–993. <https://doi.org/10.1152/physrev.00030.2016>
- Lauer, S., & Gresham, D. (2019). An evolving view of copy number variants. *Current Genetics*, 65(6), 1287–1295. <https://doi.org/10.1007/s00294-019-00980-0>
- Li, X., Venugopalan, S. R., Cao, H., Pinho, F. O., & Paine, M. L. (2014a). A model for the molecular underpinnings of tooth defects in Axenfeld-Rieger syndrome. *Human Molecular Genetics*, 23, 194–208. <http://hmg.oxfordjournals.org/content/23/1/194.full>
- Li, X., Venugopalan, S. R., Cao, H., Pinho, F. O., Paine, M. L., Snead, M. L., Semina, E. V., & Amendt, B. A. (2014b). A model for the molecular underpinnings of tooth defects in Axenfeld-Rieger syndrome. *Human Molecular Genetics*, 23(1), 194–208. <https://doi.org/10.1093/hmg/ddt411>
- Lin, C. R., Kioussi, C., O'Connell, S., Briata, P., Szeto, D., Liu, F., Izpisua-Belmonte, J. C., & Rosenfeld, M. G. (1999). Pitx2 regulates lung asymmetry, cardiac positioning and pituitary and tooth morphogenesis. *Nature*, 401(6750), 279–282. <Go to ISI>://WOS:000082678400054
- Liu, F., Chu, E. Y., Watt, B., Zhang, Y., Gallant, N. M., Andl, T., Yang, S. H., Lu, M. M., Piccolo, S., Schmidt-Ullrich, R., Taketo, M. M., Morrisey, E. E., Atit, R., Dlugosz, A. A., & Millar, S. E. (2008). Wnt/

- beta-catenin signaling directs multiple stages of tooth morphogenesis. *Developmental Biology*, 313(1), 210–224. <https://doi.org/10.1016/j.ydbio.2007.10.016>
- Liu, F., Dangaria, S., Andl, T., Zhang, Y., Wright, A. C., Damek-Poprawa, M., Piccolo, S., Nagy, A., Taketo, M. M., Diekwisch, T. G., Akintoye, S. O., & Millar, S. E. (2010). Beta-catenin initiates tooth neogenesis in adult rodent incisors. *Journal of Dental Research*, 89(9), 909–914. <https://doi.org/10.1177/0022034510370090>
- Lu, M. F., Pressman, C., Dyer, R., Johnson, R. L., & Martin, J. F. (1999). Function of Rieger syndrome gene in left-right asymmetry and craniofacial development. *Nature*, 401(6750), 276–278. <https://doi.org/10.1038/45797>
- Mucchielli, M. L., Mitsiadis, T. A., Raffo, S., Brunet, J. F., Proust, J. P., & Goridis, C. (1997). Mouse *Otx2/RIEG* expression in the odontogenic epithelium precedes tooth initiation and requires mesenchyme-derived signals for its maintenance. *Developmental Biology*, 189(2), 275–284. <https://doi.org/10.1006/dbio.1997.8672>
- O'Dwyer, E. M., & Jones, D. C. (2005). Dental anomalies in Axenfeld-Rieger syndrome. *International Journal of Paediatric Dentistry*, 15(6), 459–463. <https://doi.org/10.1111/j.1365-263X.2005.00639.x>. http://www.ncbi.nlm.nih.gov/entrez/query.fcgi?cmd=Retrieve&db=pubmed&dopt=Abstract&list_uids=16238657&query_hl=1
- Reis, L. M., Tyler, R. C., Volkmann Kloss, B. A., Schilter, K. F., Levin, A. V., Lowry, R. B., Zwijnenburg, P. J., Stroh, E., Broeckel, U., Murray, J. C., & Semina, E. V. (2012). PITX2 and FOXC1 spectrum of mutations in ocular syndromes. *European Journal of Human Genetics*, 20(12), 1224–1233. <https://doi.org/10.1038/ejhg.2012.80>
- Shin, N. Y., Yamazaki, H., Beniash, E., Yang, X., Margolis, S. S., Pugach, M. K., Simmer, J. P., & Margolis, H. C. (2020). Amelogenin phosphorylation regulates tooth enamel formation by stabilizing a transient amorphous mineral precursor. *The Journal of Biological Chemistry*, 295(7), 1943–1959. <https://doi.org/10.1074/jbc.RA119.010506>
- Tümer, Z., & Bach-Holm, D. (2009). Axenfeld-Rieger syndrome and spectrum of PITX2 and FOXC1 mutations. *European Journal of Human Genetics Ejhg.*, 17, 1527–1539. http://www.researchgate.net/profile/Zeynep_Tuemer2/publication/26279431_Axenfeld-Rieger_syndrome_and_spectrum_of_PITX2_and_FOXC1_mutations/links/54d85f940cf24647581a1fb1.pdf
- Waldron, J. M., McNamara, C., Hewson, A. R., & McNamara, C. M. (2010). Axenfeld-Rieger syndrome (ARS): A review and case report. *Special Care in Dentistry*, 30(5), 218–222. <https://doi.org/https://doi.org/10.1111/j.1754-4505.2010.00153.x>
- Yadav, M. C., de Oliveira, R. C., Foster, B. L., Fong, H., Cory, E., Narisawa, S., Sah, R. L., Somerman, M., Whyte, M. P., & Millan, J. L. (2012). Enzyme replacement prevents enamel defects in hypophosphatasia mice. *Journal of Bone and Mineral Research*, 27(8), 1722–1734. <https://doi.org/10.1002/jbmr.1619>
- Yang, Y., Wang, X., Zhao, Y., & Qin, M. (2018). A novel 4q25 microdeletion encompassing PITX2 associated with Rieger syndrome. *Oral Diseases*, 24(7), 1247–1254. <https://doi.org/10.1111/odi.12894>
- Yu, W., Sun, Z., Sweat, Y., Sweat, M., Venugopalan, S. R., Eliason, S., Cao, H., Paine, M. L., & Amendt, B. A. (2020). Pitx2-Sox2-Lef1 interactions specify progenitor oHral/dental epithelial cell signaling centers. *Development*, 147(11), dev186023. <https://doi.org/10.1242/dev.186023>
- Zacharias, A. L., & Gage, P. J. (2010). Canonical Wnt/beta-catenin signaling is required for maintenance but not activation of Pitx2 expression in neural crest during eye development. *Developmental Dynamics*, 239(12), 3215–3225. <https://doi.org/https://doi.org/10.1002/dvdy.22459>

SUPPORTING INFORMATION

Additional supporting information can be found online in the Supporting Information section at the end of this article.

How to cite this article: Yang, Y., Zhu, J., Chiba, Y., Fukumoto, S., Qin, M., & Wang, X. (2022). Enamel defects of Axenfeld-Rieger syndrome and the role of PITX2 in its pathogenesis. *Oral Diseases*, 00, 1–11. <https://doi.org/10.1111/odi.14315>